J Mater Sci (2007) 42:5736–5741
DOI 10.1007/s10853-006-0754-8

Effect of AlN particles on the corrosion behavior of Al/AlN$_P$ composites

ZhangSheng Liu · BianTao Wu · MingYuan Gu

Received: 27 November 2005 / Accepted: 3 August 2006 / Published online: 21 April 2007

Abstract The corrosion behavior of Al/AlN$_P$ composites has been examined by using potentiodynamic polarization technique in 3.5wt% NaCl solution with the pH value of 5, 8.6, and 11.6 respectively. Electrochemical impedance spectra (EIS) measurements have also been carried out to assess the long-term effects of AlN particles. It has been found that Al/AlN$_p$ composites show the increased susceptibility to pitting attack compared with the unreinforced Al, which is attributed to the micro-galvanic action between AlN particles and the matrix Al. The micro-galvanic action mainly arises as a result of hydrolysis of AlN particles. In addition, EIS measurements reveal that the corrosion mechanism of Al/AlN$_p$ composites changes a lot with increasing immersion time, which is controlled by diffusion process at last.

Introduction

Aluminum matrix composites (AMCs) have become attractive in many applications in the last few decades, since they have advantages over the conventional aluminum alloys with respect to physical or mechanical properties. There have been a significant amount of researches on the microstructure and optimization of the mechanical behavior of AMCs. However, only limited information is available concerning their corrosion characteristics in aqueous environment. Similar to Al, the predominant mode of corrosion for AMCs is pitting attack [1–3]. Studies on AMCs have shown that more pits are formed in composites than in the unreinforced Al. Corrosion studies on AMCs have focused on the effect of the reinforcement on the pitting behavior [4]. Aylor and Moran [5] found that preferential attack occurs at the reinforcement/matrix interface, which is attributed to the formation of crevices at the interfaces. This finding was also supported by Mcintyre et al. [6]. However, other studies suggested that reinforcement additions do not substantially affect the pitting attack at the matrix Al, and there is no change in the pitting potential E_{pit} and the corrosion potential E_{corr} for AMCs [7, 8]. Therefore, the effect of the reinforcement on the pitting corrosion remains unclear.

As a new type of AMCs, Al/AlN$_p$ composites have been considered for a wide range of applications. From the viewpoint of corrosion science, AlN is poor conductivity and there is no interfacial reaction between AlN particles and the matrix, so their corrosion resistance should have been good. However, AlN particles hydrolyze easily, especially in the alkaline solution. This makes the corrosion behavior of Al/AlN$_p$ composites more complex.

This work was undertaken to investigate the corrosion behavior of Al/AlN$_p$ composites and the influence of AlN particles, which was monitored by scanning electron microscopy (SEM), energy dispersive X-ray analysis (EDX) and electrochemical techniques such as potentiodynamic polarization and EIS technique.

Z. S. Liu (✉) · M. Y. Gu
State Key Lab of MMCs, Shanghai JiaoTong University,
Shanghai 200030, China
e-mail: lzsliu@sjtu.edu.cn

B. T. Wu
Department of Electrical Engineering, Shanghai Jiao Tong
University, Shanghai 200030, China

Experimental

Materials

The composites used were pure Al reinforced with 55vol%AlN particles. The composites were fabricated by vacuum infiltration technique as explained elsewhere [9, 10], and the infiltration temperature is selected as 720 °C. The AlN particle size ranged from 1 to 13 μm with a mean diameter of 6.3 μm. The composition of AlN particles was 65.8%Al, 32.6%N, 0.08%C, 1.4%O, 0.06%Fe, and 0.06%Si. Prior to electrochemical measurements, 10 × 10 × 3 mm specimens were cut from Al/AlN_p composites. They were ground to 1,000 grit and then cleaned with acetone, sealed with epoxy resin leaving one face exposed to air for the experiments.

Solutions

The electrolytes utilized in the electrochemical measurements were 3.5wt% NaCl solution with the pH values of 5, 8.6, and 11.6 respectively. The pH value of the solution was adjusted with HCl and NaOH by pH SJ-4 acidimeter.

Testing

Potentiodynamic polarization measurements

Potentiodynamic polarization tests were carried out in a classical three-electrode glass cell at 25 °C. The working electrode was the tested specimen, while the counter electrode was a platinum foil and the reference electrode was a silver–silver chloride electrode (Ag/AgCl sat. KCl) with a Luggin capillary. Polarization curves were recorded by varying the electrode potential automatically from –2 to 0 V with scan rate of 5 mVs^{-1}.

EIS measurements

AC impedance spectra were derived using a frequency response analyzer, Solartron 1260, while the tested specimen is exposed to 3.5wt% NaCl solution with the pH value of 11.6. A two-electrode system was utilized with the same Ag/AgCl electrode as reference electrode. During the impedance measurements, a sinusoidal potential of 5 mV in amplitude and a frequency sweep of 0.01 Hz to 10^6 Hz were used.

Zeta potential

Zeta potential of the hydrolysate $Al(OH)_3$ was measured using an automated micro-electrophoresis instrument. To do this, 0.01 g $Al(OH)_3$ was transferred to 100 ml of an aqueous solution. The pH value of the solution was adjusted by dropwise addition of HCl or NaOH solutions. Before the measurement, the aqueous solution was dispersed by ultrasonic for 5 min yielding a final $Al(OH)_3$ concentration of 0.1 g/l.

Surface characterization

The microstructure and the appearance of the corrosion surfaces were examined by scanning electron microscopy (SEM). The elemental composition in certain micro-area of the corrosion surfaces was analyzed using X-ray energy dispersive spectroscopy (EDS).

Results and discussion

Polarization behavior

Typical polarization curves for pure Al and Al/AlN_p composites in 3.5wt% NaCl solution with the pH value of 5, 8.6, and 11.6 are shown in Fig. 1. As it is can be seen from polarization curves, all of curves have the similar form for both the unreinforced Al and Al/AlN_p composites showing a well-defined E_{corr}, followed by a passive region. Further increase in the potential results in marked increases in the anodic current density beyond E_{pit}, which is frequently related to breakdown of the passive film. Because the solution used was not deaerated, E_{pit} is very close to E_{corr} in Fig. 1(a) for both the unreinforced Al and Al/AlN_p composites, and the passive region is narrow. However, it does not affect our present studies, since the experiment is performed only to determine the influence, subtle or otherwise, of the reinforcement on pitting behavior.

Table 1 presents the values of major electrochemical parameters for the unreinforced Al and Al/AlN_p composites in different solutions, which are evaluated from polarization plots using Tafel analysis. The present result that E_{corr} of Al/AlN_p composites is less negative than that of the unreinforced Al in same solution is in agreement with that of Jiangyun Hou et al. [11] for the same AMCs systems, where they reported 80 mV higher E_{corr} value for Al/AlN_p composites than that for unreinforced Al. Because of the different aim of the study, they simply contributed the phenomenon to the highly insulating nature of AlN particles. As far as our studies are concerned, it is found that the difference of E_{corr} value between Al/AlN_p composites and the unreinforced Al is not a constant in the different solutions. It increases from 52 mV with the pH value of 5 to 88 mV

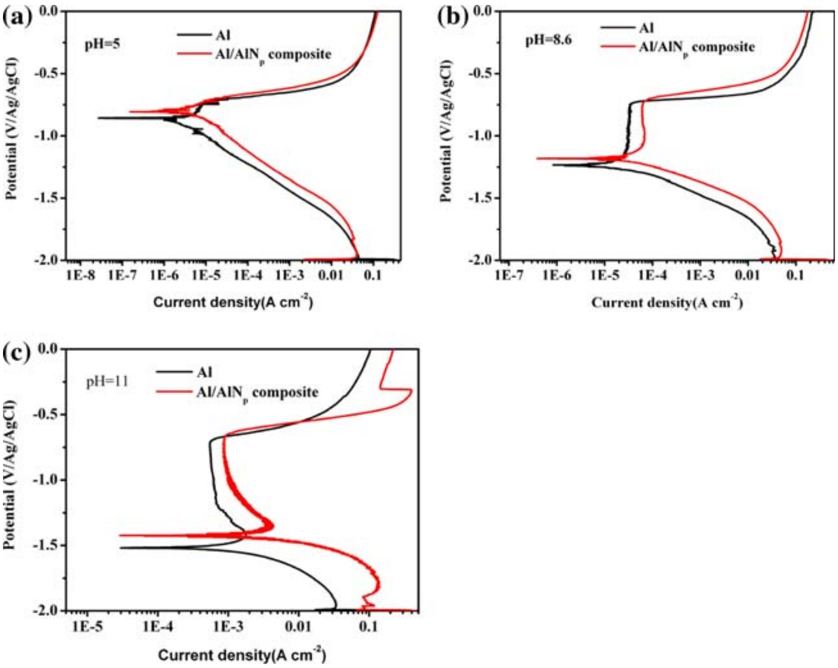

Fig. 1 polarization curves of Al and Al/AlN$_p$ composites in 3.5wt% NaCl Solution with the different pH value

Table 1 Electrochemical parameters obtained from the polarization curves

Specimen	Pure Al			Al/AlN$_p$ composites		
	E_{corr}(mV)	E_{pit}(mV)	I_{corr}(A/cm^2)	E_{corr}(mV)	E_{pit}(mV)	I_{corr}(A/cm^2)
pH = 5	–0.855	–0.755	2.009×10^{-6}	–0.803	–0.749	3.285×10^{-6}
pH = 8.6	–1.245	–0.741	3.276×10^{-6}	–1.176	–0.711	8.759×10^{-6}
pH = 11.6	–1.51	–0.702	2.081×10^{-4}	–1.422	–0.658	8.69×10^{-4}

with the pH value of 11.6, and beyond the experimental scatter of ±10 mV, suggesting that the nonconductive nature of AlN particles is not the main cause of the difference in E_{corr} value. The main cause is that AlN particles react with water according to Eq. (1), especially under the alkaline condition, which results in micro-galvanic action between hydrolyzed AlN particles and the matrix Al.

$$AlN + 4H_2O \rightarrow Al(OH)_3 + NH_4OH \tag{1}$$

In an attempt to understand this issue in some greater detail, we investigate some basics chemical property of the hydrolysate $Al(OH)_3$. Figure 2 presents Zeta potential of $Al(OH)_3$ in the solution with the different pH value. It can be seen that Zeta potential of $Al(OH)_3$ almost linearly decreases with increasing the pH value of the solution, but it remains positive value at all pHs, suggesting that high positive charges are absorbed on the surface of $Al(OH)_3$. These positive charges present in the form of H^+, which makes cathodic reactions (2) easily take place, and correspondingly hydrolyzed AlN particles

$$\frac{1}{2}O_2 + 2H^+ + 2e^- \rightarrow H_2O \tag{2}$$

exhibit the effective cathodic nature. Therefore, it is reasonable to believe that hydrolysis of AlN particles cause micro-galvanic action between AlN particles and the matrix Al.

In fact, when Al/AlN$_P$ composites specimen was left in 3.5wt% NaCl solution with the pH value of 8.6 at room temperature for 4 days, the micro-galvanic corrosion can be observed on the composites surface. Figure 3 presents the examination of the corrosion surface by SEM and EDS pattern. It can be seen that there are a lot of cluster-like white particles on the composites surface. They are believed to be hydrolyzed AlN particles, since the element oxygen, nitrogen and aluminum coexist in these particles as shown in Fig. 3. The matrix Al around these particles

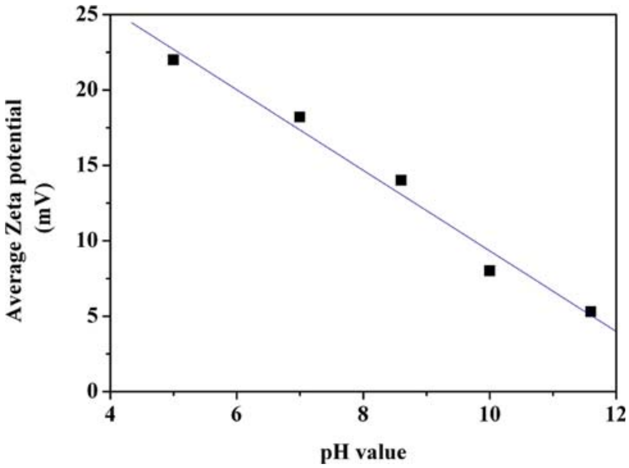

Fig. 2 Zeta potential of $Al(OH)_3$ in the solution with the different pH value

preferentially dissolves and forms micro-crevices that accelerate the pit initiation, suggesting the existence of micro-galvanic action in the interfacial area. Due to the micro-galvanic action, the surface of the pit can be divided in two parts according to their roles in the corrosion process namely: the surface of the matrix Al where the anodic dissolution takes place and the surface of hydrolyzed AlN particle where cathodic reactions occur. Herein, it is noticeable to be that when Al/AlN_p composites were immersed in 3.5wt% NaCl solution with the pH value of 2 for the same time, the pits morphology in Fig. 3(a) was not observed, which is in agreement with the fact that AlN particles does not hydrolyze in the solution with the pH value of less than 3 [12], confirming that hydrolysis of AlN particles is the main cause of the existence of micro-galvanic action.

The present results also show that E_{pit} value of Al/AlNp composites is slightly higher than that of the unreinforced Al. However, it does not mean that the susceptibility of the Al/AlN_p composites to pit initiation would be smaller than the unreinforced Al. Instead, the micro-galvanic action between the matrix Al and AlN particles makes the pit more easily initiate. As a result, I_{corr} value of Al/AlN_p composites is 4 times larger than that of the unreinforced Al in the solution with the pH value of 11.6, just as shown in Table 1.

EIS measurements

In order to investigate the long-term effect of AlN particles on the corrosion behavior of Al/AlN_p composites, the impedance technique was used as a basis for a comparative study. EIS of the unreinforced Al and Al/AlN_p composites were recorded in 3.5wt% NaCl solution with the pH value of 11.6 within 6 days respectively, and Fig. 4 shows Nyquist plots for the tested specimens.

In the case of the unreinforced Al, EIS are mainly characterized by two complete capacitive semicircles. The high-frequency semicircle is attributed to charge transfer process associated with the anodic dissolution of Al, and the low-frequency one is related to growth of a surface film [13]. With increasing immersion time, the diameters of two semicircles increase, while shapes of the plots do not change, suggesting the consistent corrosion mechanism.

In contract, Nyquist plots for Al/AlN_p composites have two distinct parts: (1) although the impedance response of Al/AlN_p composites is also characterized by two capacitive semicircles before 4 days of immersion time, they are severe depressed; (2) the depressed capacitive semicircle in low-frequency range changes over into a line inclined at 45° to the real axis after immersion time of 4 days, indicating that a diffusion process is established. As indicated in the literatures [14, 15] that depression of the capacitive semicircle is directly related with the increase in the density of pits on the surface, the depressed capacitive

Fig. 3 Surface morphology of Al/AlN_p composites and corresponding EDS pattern of hydrolyzed AlN particle

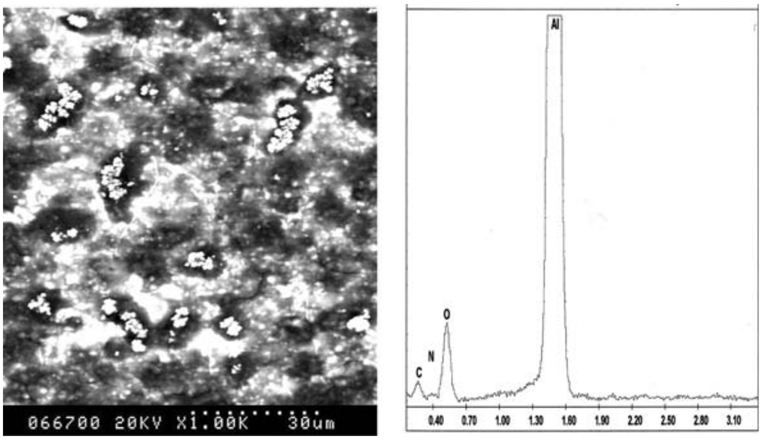

Fig. 4 Nyquist plots of (**a**) the unreinforced Al, (**b**) Al/AlN$_p$ composites

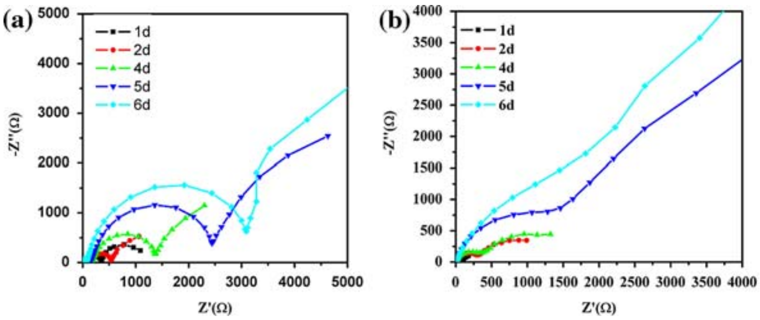

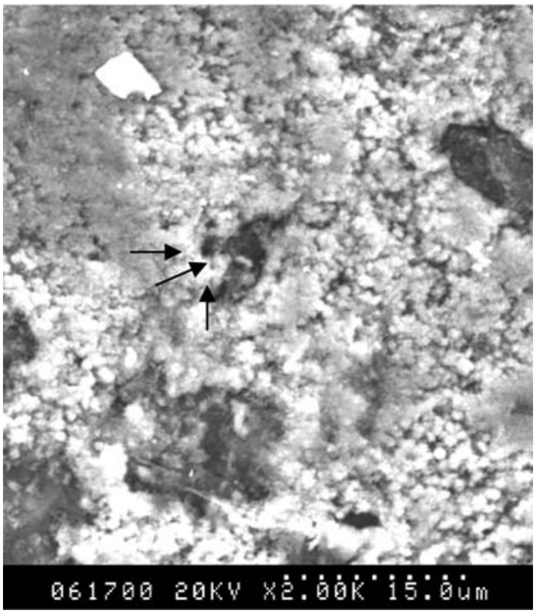

Fig. 5 Surface morphology of Al/AlN$_p$ composites with immersion time of 5 days

semicircle in this study also suggests that there are more pits in the surface of Al/AlN$_p$ composites, which is in agreement with the result of other AMCs system [7, 8]. In addition, it is also observed that the interception of the high-frequency semicircle in the real axis for Al/AlN$_p$ composites is much smaller than that for the unreinforced Al before 4 days of immersion time, suggesting more severe corrosion suffered by Al/AlN$_p$ composites. However, with the further increasing of the immersion time, more AlN particles in Al/AlN$_p$ composites hydrolyze, which can offsets some pits due to volume expansion, as shown in Fig. 5. As a result, the surface layer of Al/AlN$_p$ composites increasingly consists of hydrolyzed AlN particles and some micro-pores. It is proposed that the surface layer is not enough porous to allow a free penetration of the solution, which translates a classical barrier-type layer behavior. In this case, one can expect that the consequent corrosion process will be mainly controlled by ion diffusion, which corresponds to the long Warburg diffusion tail in the low frequency range after immersion time of 5 days in Fig. 4(b). At the same time, because of variation of corrosion mechanism, the interception of the high-frequency semicircle in the real axis increases a lot, and thus the corrosion rate of Al/AlN$_p$ composites slows down.

Conclusions

The outcome of the present work can be summarized as follows:

(1) Polarization curves reveal more susceptibility to pitting attack for Al/AlN$_p$ composites than for the unreinforced Al, which is attributed to the micro-galvanic action between AlN particles and the matrix Al.
(2) The micro-galvanic action between AlN particles and the matrix Al mainly arises as a result of hydrolysis of AlN particles.
(3) Impedance measurements reveal that the corrosion mechanism of Al/AlN$_p$ composites changes a lot with increasing immersion time. Before immersion time of 4 days, the corrosion behavior is mainly controlled by charge transfer process just like the matrix Al, while it is controlled by the diffusion process after 4 days.

Acknowledgement The authors are grateful for the financial support from the National Natural Science Foundation of China under grant No.50271043.

Reference

1. Buarzaiga MM, Thorpe SJ (1994) Corros Sci 50:176
2. Nunes PCR, Ramanathan LV (1995) Corrosion 51:610
3. Trzaskoma PP, McCafferty EM, Crowe CR (1983) J Electrochem Soc 130:1804
4. Lucas KA, Clarke H, Corrosion of Aluminum-Based Metal Matrix Composites, Research Studies Press LTD, 1993
5. Aylor DM, Moran PJ (1985) J Electrochem Soc 132:1277
6. McIntyre JF, Conrad RK, Golledge SL (1990) Corrosion 46:902
7. Trzaskoma PP (1990) Corrosion 46:402
8. Buarzaiga MM, Thorpe SJ (1994) Corrosion 50:837

9. Chung WS, Lin SJ (1996) Mat Res Bull 12:1437
10. Sahin Y, Aclar M (2003) Compos Part A-Appls 34:709
11. Hou JY, Chung DDL (1997) J Mater Sci 32:3113
12. Bowen P, Highfield JG, Mocellin A, Ring TA (1990) J Am Ceram Soc 73:724
13. EmregÜl KC, Abbas AksÜt A (2000) Corros Sci 42:2051
14. Roberge PR, Halliop E, Lenard DR, Moores JG (1993) Corros Sci 35:213
15. Conde A, de Damborenea J (1998) J Electrochimica Acta 43:849